Comparison of Magnetic Properties of MRI Contrast Media Solutions at Different Magnetic Field Strengths

Martin Rohrer, PhD, Hans Bauer, PhD,* Jan Mintorovitch, PhD,† Martin Requardt, PhD,‡ and Hanns-Joachim Weinmann, PhD**

Rationale and Objectives: To characterize and compare commercially available contrast media (CM) for magnetic resonance imaging (MRI) in terms of their relaxivity at magnetic field strengths ranging from 0.47 T to 4.7 T at physiological temperatures in water and in plasma. Relaxivities also were quantified in whole blood at 1.5 T.

Methods: Relaxivities of MRI-CM were determined by nuclear magnetic resonance (NMR) spectroscopy at 0.47 T and MRI phantom measurements at 1.5 T, 3 T, and 4.7 T, respectively. Both longitudinal (T_1) and transverse relaxation times (T_2) were measured by appropriate spin-echo sequences. Nuclear magnetic resonance dispersion (NMRD) profiles were also determined for all agents in water and in plasma.

Results: Significant dependencies of relaxivities on the field strength and solvents were quantified. Protein binding leads to both increased field strength and solvent dependencies and hence to significantly altered T_1 relaxivity values at higher magnetic field strengths.

Conclusions: Awareness of the field strength and solvent associated with relaxivity data is crucial for the comparison and evaluation of relaxivity values. Data observed at 0.47 T can thus be misleading and should be replaced by relaxivities measured at 1.5 T and at 3 T in plasma at physiological temperature.

Key Words: MRI contrast media, relaxivity, field strength dependence, comparative studies

(*Invest Radiol* 2005;40: 715–724)

Shortly after the development and market introduction of magnetic resonance imaging contrast media (MRI-CM; gadolinium diethylenetriaminepentaacetic acid [Gd-DTPA], MAGNEVIST), their use became a worldwide established, powerful tool for improved medical diagnosis with MRI.[1–5] After the first marketing authorization of Gd-DTPA (MAGNEVIST) in the United States, Europe, and Japan in 1988, other Gd-based chelates (eg, DOTAREM,[6] OMNISCAN,[7,8] PROHANCE,[9,10] OPTIMARK,[11] GADOVIST[12,13]) were introduced to the market. Today, contrast media are applied in approximately 30% of all MRI procedures.

Although the dominance of extracellular, low molecular-mass Gd chelates such as Gd-DTPA still persists, a number of novel and more specific MRI-CM containing other metals than Gd (Mn chelates or iron oxide particles) also have been introduced.[14–17] The use of Mn as a paramagnetic center was first introduced in Mn-DPDP (TESLASCAN).[18,19] MRI-CM based on coated superparamagnetic iron oxide (SPIO) nanoparticles such as FERIDEX/ENDOREM and RESOVIST have been developed and marketed. The SPIO substances often are referred to as "negative contrast agents" because of their strong susceptibility effects, which make them most suitable for T_2- and T_2*-weighted sequences. The paramagnetic Gd-containing MRI-CM, on the other hand, are sometimes named "positive contrast agents" based on their effective T_1-shortening characteristics, which provide an increased signal intensity in T_1-weighted sequences.

The efficacy of MRI contrast agents is not just determined by their pharmacokinetic properties (distribution and time dependence of their concentration in the area of interest) but also by their magnetic properties, described by their T_1- and T_2-relaxivities. Various factors influence these relaxivities. In the case of paramagnetic metal chelates, the paramagnetic center of the metal chelate directly interacts with the protons of the surroundings ("inner-sphere effects"), which is quantitatively described by the Solomon-Bloembergen-Morgan equations,[20] containing field-/frequency-dependent contributions from dipolar and scalar contact interactions. Motion factors (rotation, water exchange rates) are accounted for via the correlation times. Comprehensive descriptions and reviews on relaxation theory, including further contributions ("outer-sphere effects," diffusion) can be found, for instance, in the reviews by Lauffer and coworkers or Bertini and coworkers.[21–24] Detailed theoretical descriptions become further complex, when MRI-CM are considered in vivo, because the properties of the agent depend on the different physiological environments (eg, blood, interstitial fluids, intracellu-

Received December 1, 2004, and accepted for publication, after revision, August 2, 2005.

From *Schering AG, Berlin, Germany; †Berlex Laboratories, Montville, New Jersey; and ‡Siemens Medical Solutions, Erlangen, Germany.

Reprints: Martin Rohrer, PhD, Global Business Unit Diagnostic Imaging, Schering AG, Muellerstrasse 178, 13342 Berlin, Germany. E-mail: Martin.Rohrer@Schering.de.

ISSN: 0020-9996/05/4011-0715

lar space). Another factor that also should be taken into consideration is the binding of the contrast agent to macromolecules in the blood (protein binding). This property has been described in detail elsewhere for contrast agents specifically designed to bind to proteins (eg, gadolinium benzyloxypropionictetraacetate [Gd-BOPTA], gadolinium ethoxybenzyl diethylenetriaminepentaacetic acid [Gd-EOB-DTPA], and MS-325).[22,25–28] The pharmacokinetic properties of the CM (eg, hepatobiliary sequestration, prolonged blood half-life) and the degree of relaxation rate enhancement are affected by protein binding. The concentration dependence of relaxivity, which results from the protein binding of these MRI-CM, requires awareness of the concentration, at which the relaxivity data were measured.[29]

For all commercially available MRI-CM, relaxivities are published and listed in the respective package inserts. However, the most commonly used field strength for relaxation measurements (0.47 T) is different from the currently most frequently used field strength of clinical MRI instruments (1.5 T). Hence, the purpose of this study is to compare the relaxivities of MRI-CM at different magnetic field strengths. The measurements were performed in water and in blood plasma at 0.47 T, 1.5 T, 3 T, and 4.7 T, as well as in whole blood at 1.5 T.

In the literature, relaxivities and their field strength dependencies have been discussed frequently, mostly in the context of specific and practical concerns such as the associated dose dependence,[30–34] specific applications of contrast-enhanced (CE) MRI,[35–44] or comparison of a few different MRI-CM.[45–48] This article intends to complement the existing literature by providing an overview on relaxivity data of all commercially available MRI-CM, measured under comparable conditions at different magnetic field strengths.

MATERIALS AND METHODS

Substances and Solvents

All currently commercially available contrast agents were used as supplied by the manufacturers and diluted with distilled water or plasma. In addition, 4 compounds currently (ie, at the time of article submission) in different stages of development by Schering AG and its collaboration partners also were included. All investigated MRI-CM are listed in Table 1 together with their short name as well as their generic name (International Nonproprietary Name [INN]).

If a linear relationship between relaxation rates and CM concentration is assumed, the relaxivity can, in principle, be determined from a single concentration, if the relaxation rate of the solvent is known. All nuclear magnetic resonance dispersion (NMRD) profiles rely on this assumption. However, the accuracy of any relaxivity determination depends on the number of concentrations at which the relaxation rates were measured.

The goal to investigate all commercially available CM in different solvents and at several field strengths within a reasonable time, restricted the number of concentrations that could be measured for each MRI-CM. The relaxation times of solutions containing Gd and Mn chelates were measured at the concentrations of 0.25 and 0.50 mmol/L. The SPIOs were additionally measured at 0.10 mmol/L. This approach resulted in 31 samples to be measured per solvent and field strength. Consequently, a total of 248 individual data analysis had to be conducted for the 2 solvents and 4 field strengths.

For protein-binding CM, exhibiting at least 2 different relaxing specimen in protein containing solvents (biophysical states), relaxivity values need to be considered together with the chosen concentration range. In compliance with the "Recommendations for the Nomenclature of MR Imaging Contrast Agent Terms,"[29] these compounds also can be specified by single relaxivity values.

The advantage of a comparative investigation on a large number of MRI-CM with such an experimental approach is hence complemented by the limitation that, because of the large amount of samples investigated at several magnetic field strengths and in different solvents, the individual linearities of relaxation rates versus concentration could not be verified by further relaxation rate measurements in a wider concentration range. Thus, caution is advisable with regard to possible errors because of potential nonlinear concentration

TABLE 1. Investigated MRI Contrast Media

Short Name or Internal Code	Generic Name (INN)	Trade Name(s)	Company
Gd-DTPA	Gadopentetate dimeglumine	MAGNEVIST	Schering
Gd-DO3A-butrol	Gadobutrol	GADOVIST	Schering
Gd-HP-DO3A	Gadoteridol	PROHANCE	Bracco
Gd-BOPTA	Gadobenate dimeglumine	MULTIHANCE	Bracco
Gd-DOTA	Gadoterate meglumine	DOTAREM	Guerbet
Gd-DTPA-BMA	Gadodiamide	OMNISCAN	Amersham
Mn-DPDP	Mangafodipir trisodium	TESLASCAN	Amersham
Gd-DTPA-BMEA	Gadoversetamide	OPTIMARK	Tyco Healthcare
SH U 555 A	Ferucarbotran	RESOVIST	Schering
AMI-25	Ferumoxide	FERIDEX/ENDOREM	Berlex/Guerbet
SH L 643 A (Gadomer)	Gadodenterate	N/A	Schering
MS-325	Gadofosveset trisodium	N/A	Epix/Schering
Gd-EOB-DTPA	Gadoxetic acid, disodium	PRIMOVIST	Schering
SH U 555 C	Ferucarbotran	N/A	Schering

dependencies of relaxation rates, in particular for concentration ranges far from the investigated values.

All solutions for relaxivity measurements were prepared in nonsterile bovine plasma (Kraeber GmbH, Pharmaceutical Raw Materials, Ellerbek, Germany, with a specified total protein concentration of 7.0–9.0 g/dL; corresponding to an albumin concentration of 0.64 to 0.82 mmol/L, assuming an albumin content of 60% within the total protein content and a molecular weight of 66000 for bovine albumin), in distilled water (sterile, deionized, resistance >16 MΩ cm, Millipore GmbH, Schwalbach, Germany) and in canine blood (pooled from 25 beagles, heparin added). The metal concentration of the solutions containing Gd, Mn, and Fe were verified by Inductively Coupled Plasma Atomic Emission Spectrometry (ICP-AES; Minitorch 3410; ARL, Lausanne, Switzerland) and found to be accurate within ±5%.

Measurement of Relaxation Curves

Measurements at 0.47 T were performed using a Minispec PC-20 spectrometer (Bruker Analytik, Karlsruhe, Germany) operating at a proton frequency of 20 MHz and a preset temperature of 40°C. The standard software of the Minispec (EDM 510 A for T_1) was a 2-pulse inversion-recovery (IR) sequence with a fixed relaxation delay of at least $5 \times T_1$. The variable TI was calculated automatically, based on an estimated T_1 value (T_{1e}), and ranged from $0.04 \times T_{1e}$ to $5.12 \times T_{1e}$ in 8 steps. The T_2 measurements were done by using the corresponding Carr-Purcell-Meiboom-Gill (CPMG) software (EDM 610), applying relaxation delays of $5 \times T_1$, with the T_1 values as determined above. All samples were measured individually at 0.47 T.

Measurements at 1.5 T were conducted using standard imaging protocols on a MAGNETOM-type MRI scanner (Siemens Medical Solutions, Erlangen, Germany). Measurements at 3 T were performed with a MAGNETOM TRIO whole-body MRI scanner (Siemens Medical Solutions, Erlangen, Germany). For sequence parameters at 1.5 T and at 3 T, see below.

The sample tubes (10 mm inner diameter) were positioned in 2 rows of 15 and 16 tubes, in a styrene box filled with water. The temperature of the water was equilibrated at 37°C for 1 h and manually controlled throughout the duration of the measurements. At each field strength, the entire imaging protocols were completed in approximately 10 minutes.

Measurements at 4.7 T were performed using an INOVA MRI scanner (Varian Inc., Palo Alto, CA). Up to 6 samples were placed in a row in a plastic holder. The temperature was adjusted to 37°C with heated air and controlled by 2 test tubes containing a thermocouple. Spectra in the presence of the readout gradient only were recorded, instead of acquisition of the usual 2D data sets.

Relaxation curves for T_1 calculations were obtained by 2D imaging with an inversion-recovery turbo spin-echo (IR-TSE) pulse sequence. At 1.5 T, the sequence was either run with a fixed sequence repetition time (TR) of 3 seconds, or with a constant relaxation delay of 1.5 seconds after the registration of the last echo (variable TR). For T_1 values in the range of 100 milliseconds to 600 milliseconds, both protocols resulted in equivalent values, but the variable TR measurement saved approximately 50% of imaging time and hence allowed for higher temperature stability. At 3 T and 4.7 T, constant delays (TR-TI) of 1.5 seconds and 3 seconds were applied. The shortest possible echo-time values (TEs) were chosen: 6.9 milliseconds at 1.5 T, 7.3 milliseconds at 3 T, and 6 milliseconds at 4.7 T. The effective echo train lengths (ETL) were 17, 7, and 1, respectively. The following inversion times were applied: at 1.5 T: 30, 60, 90, 120, 150, 250, 400, 600, 800, 1200, 1600, and 2000 milliseconds; at 3 T: 40, 60, 70, 100, 140, 160, 200, 250, 300, 600, 800, 1000, 1500, and 1700 milliseconds; and at 4.7 T: 10, 50, 100, 150, 200, 300, 400, 500, 600, 800, 1000, 2000, 4000, 8000, and 15000 milliseconds. The inversion times at 1.5 T and 3 T were chosen to optimize the sequence to measure T_1 values in the range from 100 milliseconds to 600 milliseconds, corresponding to the estimated T_1 range of all relaxation times of CM containing solutions. At 4.7 T, according to faster data acquisition without phase encoding, longer TI values could be additionally applied. As an example, the T_1 relaxation curves obtained for MAGNEVIST at 1.5 T, 3 T and at 4.7 T, are shown in Figure 1. For details of the fit procedure, see the section "Calculation of Relaxation Times."

The experimental matrices for the phantom measurements were 176×256 (1.5 T), 128×256 (3 T), and 1×256 (4.7 T, no phase encoding). The reconstructed matrices were 256×256 pixel at 1.5 T and at 3 T and 1D spectra of 256 pixels at 4.7 T. Relaxation curves for T_2 calculation were obtained by a multiecho spin-echo sequence (ME-SE) recording one image for each echo time. Echo train lengths were 32 with an echo spacing of 7 milliseconds (1.5 T) and 11.5 milliseconds (3 T), respectively. At 4.7 T the ETL ranged from 64 to 1200 with an echo spacing of 4.5 milliseconds.

NMRD

In addition to the relaxivity measurements, NMRD profiles were recorded with a field-cycling relaxometer (Spinmaster FFC-2000, Stelar, Mede, Italy), operating at a frequency range of 0.01 to 70 MHz, corresponding to a magnetic field range of 0.23 mT to 1.64 T. All NMRD measurements were recorded at a temperature of 30°C and at a single concentration for each MRI-CM between 1 mmol/L (Gadomer) and 4 mmol/L (SH U 555 C). The temperature setting of 30°C and the technically limited magnetic field range were different to the other measurements. Hence, results from NMRD profiles were not quantitatively accounted for the data presented in the tables.

Calculation of Relaxation Times

Using MRI, the mean signal intensity (SI) of each sample was determined individually by evaluation of the respective region of interest (ROI) within the phantom measurements. The longitudinal relaxation times T_1 were obtained by fitting the experimental SI of the IR-TSE sequence to the absolute values of the calculated SI(TI), given by the basic equation:

$$SI(TI) = |SI_{inf}[1 - (1 - k) \cdot e^{-TI/T_1}]| \qquad (1a)$$

where SI(TI) denotes the SI as a function of TI, SI_{inf} is the SI from the spin system in thermal equilibrium, and k corre-

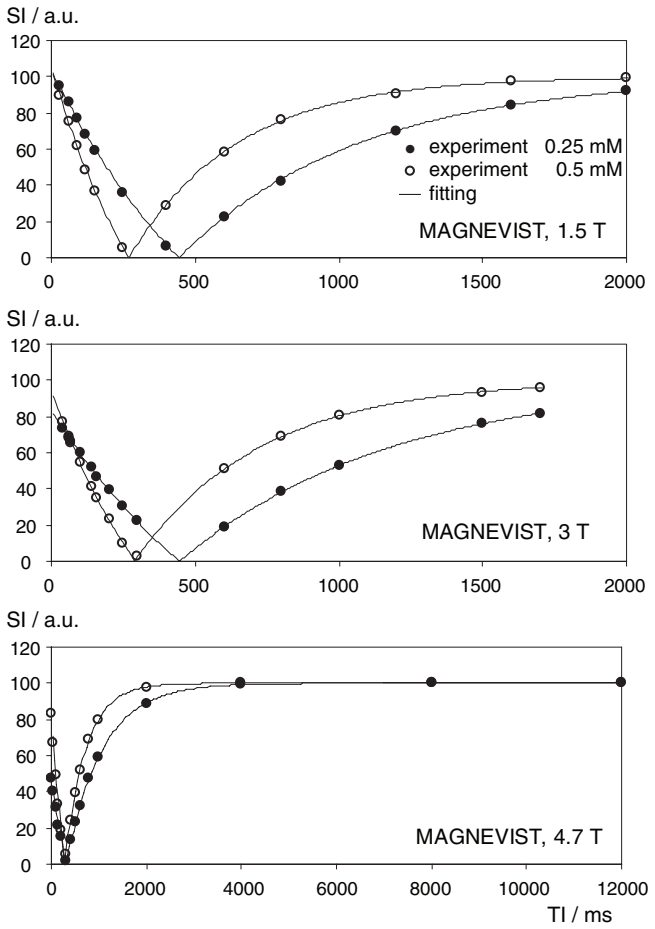

FIGURE 1. Relaxation curves obtained at 1.5 T, 3 T, and 4.7 T in plasma at 0.25 mM and 0.5 mM. Three-parameter fitting of normalized experimental signal intensities as a function of TI. As an example, the T_1 relaxation curves of a Gd chelate (MAGNEVIST) at 0.25 mM and 0.5 mM concentration in bovine plasma, obtained at 37°C at 1.5 T (top), 3 T (center) and at 4.7 T (bottom) are shown. The standard errors for the T_1 fittings at 0.5 mM concentration were ±0.88%, ±0.71% and ±0.32%, respectively. They were determined and taken into account for each sample measurement individually. For details, see text.

sponds to the cosine of the excitation angle of the inversion pulse ($\cos(\beta)$). Eq. (1a) is strictly valid for inversion recovery sequences with full relaxation ($TR \gg T_1$). For IR sequences with faster repetition ($TR \approx T_1$), Eq. (1a) still holds true, if the correction k is modified to:

$$k = \cos(\beta)\frac{M_{SS}}{M_{inf}} \qquad (1b)$$

taking into account the steady-state magnetization (M_{SS}), which is a fraction of the magnetization at thermal equilibrium (M_{inf}). M_{SS} only depends on the delay after the signal registration (TD). Hence, TD is to be kept constant and can be even shorter than T_1 (fast inversion recovery sequence), allowing the obtainment of a relaxation curve in a shorter total acquisition time compared with the measurement using a constant TR with $TR \gg T_1$.[49] Furthermore, the condition $TE \ll T_1$ must be fulfilled and the excitation pulse must be close to 90°. In Figure 1, calculated relaxation curves are depicted for MAGNEVIST in plasma at 1.5 T, 3 T, and 4.7 T.

The transverse relaxation times T_2 were determined by fitting the experimental SI of the ME-SE sequence to the basic equation:

$$SI(TE) = SI_0 \cdot e^{-TE/T_2} + SI_{noise} \qquad (2)$$

where SI(TE) denotes the SI as a function of TE and SI_0 corresponds to the steady-state SI; SI_{noise} is the baseline noise level, taking into account that the SI in MRI cannot vanish because of the absolute value mode for image calculation.

The basic assumptions for the validity of Eqs. (1) and (2) are described elsewhere[50,51] and include that the correlation time τ_C is short compared with the relaxation times: $\tau_C < T_i$ (i = 1, 2) and that the underlying correlation function is of a typical exponential shape.

These conditions for the obtainment of single relaxation rates with monoexponential decay functions (fast exchange limit) can be strictly predicted only for the relaxation time measurements in water. In solutions containing proteins which strongly interact with the MRI-CM, contributions from slow exchange limit will alter the situation. This is sometimes referred to as the compartmentalization effect.[52] As can be rationalized by an altered τ_C in the protein bound state, deviations from a mono exponential decay become possible. If in such cases a single relaxation time (apparent T_i) is calculated, the result depends on the experimental conditions including the protein concentration.[53]

Eq. (1) was fitted with 3 parameters (SI_{inf}, k, T_1) using the Solver Add-In of MS-Excel™. The errors of these parameters were determined individually (see the section "Error Estimation"). For Eq. 2 only a 2-parameter fit (SI_0, T_2) was performed, because the noise baseline (SI_{noise}) is a constant technical parameter, that could be determined from the experimental SI after full relaxation ($TE > 5 \times T_2$).

Calculation of Relaxivities

Relaxivities (r_1 and r_2) are generally defined as the slope of the linear regression generated from a plot of the measured relaxation rate ($1/T_i$, where i = 1, 2) versus the concentration of the MRI-CM:

$$\frac{1}{T_i} = \frac{1}{T_{i(0)}} + r_i \cdot [CM] \qquad (3a)$$

$$\left(\frac{1}{T_i} - \frac{1}{T_{i(0)}}\right) = r_i \cdot [CM] \qquad (3b)$$

where T_i denotes the longitudinal (T_1) or transverse (T_2) relaxation times of a solution containing CM and $T_{i(0)}$ the relaxation times of the solvent without MRI-CM. The difference of the relaxation rates (Eq. 3b) is referred as $\Delta(1/T_i)$.

To keep the measurement time short and hence to avoid temperature drifts that would affect the measured relaxation times, the sequence parameters (TR, TI) were optimized for T_1 relaxation times in the range of 100 to 600 milliseconds. Thus, the determination of the solvent relaxation rate ($1/T_{1(0)}$), required for Eq. (3), was intrinsically less accurate due to the sequence parameters, than was the case for the relaxation rates ($1/T_1$) obtained for the CM solutions. Instead of applying a linear regression with 2 variable parameters, ie, $1/T_{1(0)}$ and r_1 for each CM individually, as given in Eq. (3a), the following procedure was applied: taking advantage of the fact that the actual solvent relaxation rate was the same for all CM solutions measured simultaneously, the number of variable parameters, ie, 2 × n (where n is the number of different CM), could be reduced to n + 1. This was achieved by linking the individual slope determinations (relaxivities) with a global determination of $1/T_{1(0)}$ by applying Eq. (3b) as shown in Figure 2. The experimentally determined solvent relaxation rate $1/T_{1(0)}$ was subtracted as a starting value from the CM relaxation rates prior to the linear regression analysis. In the analysis, the global $1/T_{1(0)}$ was varied together with all relaxivities. The best fit for the solvent relaxation rate was obtained for the minimum sum of the relative errors of all relaxivities. The relative error was then given as the ratio of the error of the slope divided by the slope.

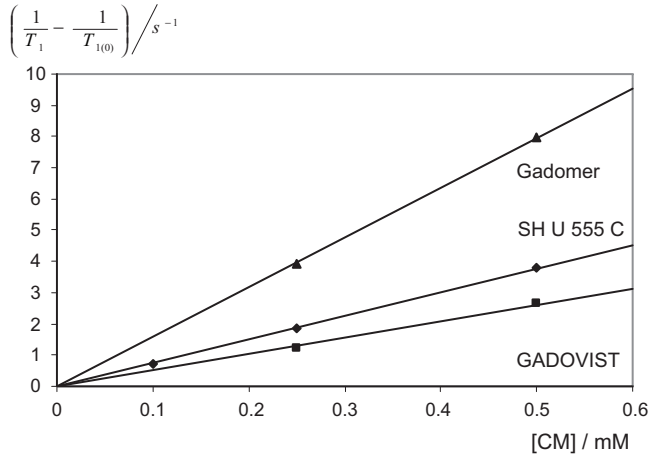

FIGURE 2. Determination of r_1 of Gadomer, RESOVIST and GADOVIST at 1.5 T in plasma. Plot of the differences of relaxation rates $\Delta(1/T_1)$ versus the concentration of 3 examples of MRI-CM (Gadomer, GADOVIST, SH U 555 C) and their linear regressions. These measurements were performed at 1.5 T in bovine plasma at 37°C. The individual accuracy ranges of relaxivity values were determined for the 0.5 mM concentration, as explained in the text.

Importantly, the solvent relaxation rate was not an individual fit parameter within the single slope determinations, but always applied to all linear regressions simultaneously. This procedure is certainly justified, since during the respective measurement the solvent relaxation rate was the same for all solutions. The final solvent relaxation rates calculated by this procedure (except for 0.47 T) are given in Table 2.

Error Estimation

To obtain relaxation times T_1 according to Eq. (1), a 3-parameter fit was applied to the experimental SI versus TI curves, as described previously and shown in Figure 1. Standard errors were determined for each T_1 value from the variance-covariance matrix, the sum of squared deviations and the degree of freedom, individually. The degree of freedom was given by the difference between the number of data points and the number of variable parameters. Typically, for T_1 values in the range of 100 to 600 milliseconds, these errors were in the range of ±0.2 to ±1%, depending on field strength, solvent and CM concentration.

The absolute errors of the differences of T_1 relaxation rates ($\Delta(1/T_1)$) were calculated according to the Gaussian law of error propagation as given in Eq. (4a):

$$\mathrm{err}_{\Delta(1/T_i)} = \sqrt{(\mathrm{err}_{1/T_i})^2 + (\mathrm{err}_{1/T_{i(0)}})^2} \qquad (4a)$$

where err_{1/T_i} denotes the absolute error of the relaxation rate ($i = 1$ for T_1) with CM and $\mathrm{err}_{1/Ti(0)}$ the absolute error of the relaxation rate of the solvent, as given in Table 2.

The error of the relaxivity err_{ri} for one sample, ie, $r_i = \Delta(1/T_i)/[CM]$, was obtained by Eq. (4b):

$$\frac{\mathrm{err}_{r_i}}{r_i} = \sqrt{\left(\frac{\mathrm{err}_{\Delta(1/T_i)}}{\Delta(1/T_i)}\right)^2 + \left(\frac{\mathrm{err}_{[CM]}}{[CM]}\right)^2} \qquad (4b)$$

where [CM] denotes the concentration of CM, and *err* are the respective absolute errors.

The calculated errors for the samples containing the highest CM concentration were regarded as the maximum possible errors for the relaxivities. Since these maximum possible errors are directly related to the respective concentration (0.5 mmol/L), they are also legitimate error values for CM exhibiting nonlinearity, solely for the chosen concentration.

TABLE 2. Relaxation Rates* of Investigated Solvents at 37°C†

	0.47 T†		1.5 T		3 T		4.7 T	
	$1/T_{1(0)}$	$1/T_{2(0)}$	$1/T_{1(0)}$	$1/T_{2(0)}$	$1/T_{1(0)}$	$1/T_{2(0)}$	$1/T_{1(0)}$	$1/T_{2(0)}$
Water	0.270 ± 0.001	0.313 ± 0.001	0.24 ± 0.03	0.8 ± 0.1	0.2 ± 0.1	0.32 ± 0.06	0.22 ± 0.01	0.38 ± 0.03
Plasma	0.667 ± 0.003	1.887 ± 0.006	0.63 ± 0.06	2.4 ± 0.2	0.44 ± 0.06	2.9 ± 0.4	0.37 ± 0.02	4.4 ± 0.2
Blood			0.8 ± 0.1	4.4 ± 0.2				

*Values in s^{-1} (see text for details).
†At 0.47 T: measured separately at 40°C.

The final accuracy ranges of the relaxivities r_1, as determined by this procedure and listed in Tables 3 to 5, include the concentration error of ±5%.

T_2 was obtained by a 2-parameter fit according to Eq. (2) as described previously. Individual error calculation for T_2 relaxation was done similar to the procedure described for T_1. The lowest errors for T_2 were found in plasma at 4.7 T, lying well below 1%, except for the SPIO. The highest error values of up to 20% were found in water at 1.5 T. The final accuracy ranges of the relaxivities r_2, were found according to the same procedure as described previously for r_1 and are also listed individually in Tables 3 to 5.

RESULTS AND DISCUSSION

Relaxivities in Water

The generated NMRD profiles of 3 selected contrast media (Fig. 3) illustrate the field strength dependencies of their relaxivities. Although the magnetic field range of the relaxometer was restricted to an upper limit of about 1.65 T,

TABLE 3. Relaxivities* of Investigated Contrast Media in Water at 37°C

Trade Name or Internal Code	0.47 T†		1.5 T		3 T		4.7 T	
	r_1	r_2	r_1	r_2	r_1	r_2	r_1	r_2
MAGNEVIST	3.4 (3.2–3.6)	4.0 (3.8–4.2)	3.3 (3.1–3.5)	3.9 (2.8–5.0)	3.1 (2.8–3.4)	3.7 (3.4–4.0)	3.2 (3.0–3.4)	4.0 (3.8–4.2)
GADOVIST	3.7 (3.5–3.9)	5.1 (4.8–5.4)	3.3 (3.1–3.5)	3.9 (3.1–4.7)	3.2 (2.9–3.5)	3.9 (3.6–4.2)	3.2 (3.0–3.4)	3.9 (3.7–4.1)
PROHANCE	3.1 (2.9–3.3)	3.7 (3.5–3.9)	2.9 (2.7–3.1)	3.2 (2.5–3.9)	2.8 (2.6–3.0)	3.4 (3.1–3.7)	2.8 (2.7–2.9)	3.7 (3.5–3.9)
MULTIHANCE	4.2 (3.9–4.4)	4.8 (4.6–5.0)	4.0 (3.8–4.2)	4.3 (3.8–4.8)	4.0 (3.7–4.3)	4.7 (4.4–5.0)	4.0 (3.8–4.2)	5.0 (4.7–5.3)
DOTAREM	3.4 (3.2–3.6)	4.1 (3.9–4.3)	2.9 (2.7–3.1)	3.2 (2.5–3.9)	2.8 (2.6–3.0)	3.3 (3.0–3.6)	2.8 (2.7–2.9)	3.7 (3.5–3.9)
OMNISCAN	3.5 (3.3–3.7)	3.8 (3.6–4.0)	3.3 (3.1–3.5)	3.6 (3.0–4.2)	3.2 (2.9–3.5)	3.8 (3.5–4.1)	3.3 (3.1–3.5)	4.1 (3.9–4.3)
TESLASCAN	1.9 (1.8–2.0)	2.1 (2.0–2.2)	1.6 (1.5–1.7)	2.1 (1.4–2.8)	1.5 (1.3–1.7)	2.3 (2.0–2.6)	1.6 (1.5–1.7)	2.7 (2.6–2.8)
OPTIMARK	4.2 (4.0–4.4)	5.2 (4.9–5.5)	3.8 (3.6–4.0)	4.2 (3.5–4.9)	3.6 (3.3–3.9)	4.5 (4.2–4.8)	3.8 (3.6–4.0)	4.7 (4.5–4.9)
RESOVIST	20.6 (19.5–21.7)	86 (82–90)	8.7 (8.2–9.2)	61 (54–68)	4.6 (4.3–4.9)	143 (132–154)	2.8 (2.7–2.9)	176 (167–185)
FERIDEX/ ENDOREM	27 (26–28)	152 (144–160)	4.7 (4.4–5.0)	41 (39–43)	4.1 (3.8–4.4)	93 (87–99)	2.3 (2.2–2.4)	105 (100–110)
Gadomer	16.5 (15.7–17.3)	17 (16–18)	17.3 (16.4–18.2)	22 (21–23)	13.0 (12.3–13.7)	23 (22–24)	9.1 (8.6–9.6)	22 (21–23)
MS-325	5.8 (5.5–6.1)	6.7 (6.4–7.0)	5.2 (4.9–5.5)	5.9 (5.3–6.5)	5.3 (5.0–5.6)	6.1 (5.7–6.5)	5.5 (5.2–5.8)	6.9 (6.5–7.3)
PRIMOVIST	5.3 (5.0–5.6)	6.2 (5.9–6.5)	4.7 (4.5–4.9)	5.1 (4.5–5.7)	4.3 (4.0–4.6)	5.5 (5.2–5.8)	4.9 (4.7–5.1)	6.3 (6.0–6.6)
SH U 555 C	23.9 (22.7–25.1)	54 (51–57)	13.2 (12.5–13.9)	44 (41–47)	7.3 (6.9–7.7)	57 (54–60)	4.3 (4.1–4.5)	66 (63–69)

*Values in L $mmol^{-1}$ s^{-1}.
†Measured at 40°C (see text for details).

TABLE 4. Relaxivities* of Investigated Contrast Media in Plasma at 37°C

Trade Name or Internal Code	0.47 T†		1.5 T		3 T		4.7 T	
	r_1	r_2	r_1	r_2	r_1	r_2	r_1	r_2
MAGNEVIST	3.8 (3.6–4.0)	4.1 (3.9–4.3)	4.1 (3.9–4.3)	4.6 (3.8–5.4)	3.7 (3.5–3.9)	5.2 (4.3–6.1)	3.8 (3.6–4.0)	4.8 (4.3–5.3)
GADOVIST	6.1 (5.8–6.4)	7.4 (7.0–7.8)	5.2 (4.9–5.5)	6.1 (5.2–7.0)	5.0 (4.7–5.3)	7.1 (6.2–8.0)	4.7 (4.5–4.9)	5.9 (5.4–6.4)
PROHANCE	4.8 (4.6–5.0)	6.1 (5.8–6.4)	4.1 (3.9–4.3)	5.0 (4.2–5.8)	3.7 (3.5–3.9)	5.7 (4.8–6.6)	3.7 (3.5–3.9)	5.8 (5.3–6.3)
MULTIHANCE	9.2 (8.7–9.7)	12.9 (12.2–13.6)	6.3 (6.0–6.6)	8.7 (7.8–9.6)	5.5 (5.2–5.8)	11.0 (10.0–12.0)	5.2 (4.9–5.5)	10.8 (10.1–11.5)
DOTAREM	4.3 (4.1–4.5)	5.5 (5.2–5.8)	3.6 (3.4–3.8)	4.3 (3.4–5.2)	3.5 (3.3–3.7)	4.9 (4.0–5.8)	3.3 (3.1–3.5)	4.7 (4.2–5.2)
OMNISCAN	4.4 (4.2–4.6)	4.6 (4.4–4.8)	4.3 (4.0–4.6)	5.2 (4.2–6.2)	4.0 (3.8–4.2)	5.6 (4.7–6.5)	3.9 (3.7–4.1)	5.3 (4.8–5.8)
TESLASCAN	3.6 (3.4–3.8)	4.3 (4.1–4.5)	3.6 (3.4–3.8)	7.1 (5.7–8.5)	2.7 (2.5–2.9)	9.3 (8.3–10.3)	2.2 (2.1–2.3)	9.4 (8.8–10.0)
OPTIMARK	5.7 (5.4–6.0)	6.6 (6.3–6.9)	4.7 (4.4–5.0)	5.2 (4.3–6.1)	4.5 (4.2–4.8)	5.9 (5.0–6.8)	4.4 (4.2–4.6)	5.9 (5.4–6.4)
RESOVIST	15 (14–16)	101 (96–106)	7.4 (7.0–7.8)	95 (86–104)	3.3 (3.1–3.5)	160 (140–180)	1.7 (1.6–1.8)	118 (110–126)
FERIDEX/ ENDOREM	—	—	4.5 (4.2–4.8)	33 (31–35)	2.7 (2.5–2.9)	45 (42–48)	1.2 (1.1–1.3)	25 (24–26)
Gadomer	19 (18–20)	23 (22–24)	16 (15–17)	19 (18–20)	13 (12–14)	25 (23–27)	9.1 (8.6–9.6)	23 (22–24)
MS-325	28 (27–29)	40 (38–42)	19 (18–20)	34 (32–36)	9.9 (9.4–10.4)	60 (56–64)	6.9 (6.6–7.2)	60 (57–63)
PRIMOVIST	8.7 (8.3–9.1)	13 (12–14)	6.9 (6.5–7.3)	8.7 (7.8–9.6)	6.2 (5.9–6.5)	11 (10–12)	5.9 (5.6–6.2)	12 (11–13)
SH U 555 C	22.3 (21.2–23.4)	99 (94–104)	10.7 (10.1–11.3)	38 (36–40)	5.6 (5.3–5.9)	95 (86–104)	2.9 (2.8–3.0)	69 (66–72)

*Values in L $mmol^{-1}$ s^{-1}.
†Measured at 40°C (see text for details).

TABLE 5. Relaxivities* of Investigated Contrast Media in Blood at 37°C

	1.5 T	
Trade Name or Internal Code	r_1	r_2
MAGNEVIST	4.3 (4.0–4.6)	4.4 (3.6–5.2)
GADOVIST	5.3 (5.0–5.6)	5.4 (4.6–6.2)
PROHANCE	4.4 (4.1–4.7)	5.5 (5.0–6.0)
MULTIHANCE	6.7 (6.3–7.1)	8.9 (7.9–9.9)
DOTAREM	4.2 (3.9–4.5)	6.7 (6.0–7.4)
OMNISCAN	4.6 (4.3–4.9)	6.9 (5.5–8.3)
TESLASCAN	5.2 (4.9–5.5)	8.9 (8.2–9.6)
OPTIMARK	5.2 (4.9–5.5)	6.0 (5.4–6.6)
RESOVIST	8.0 (7.5–8.5)	77 (71–83)
FERIDEX/ENDOREM	7.0 (6.6–7.4)	66 (61–71)
Gadomer	17 (16–18)	22 (21–23)
MS-325	19 (18–20)	37 (35–39)
PRIMOVIST	7.3 (6.9–7.7)	9.1 (8.2–10.0)
SH U 555 C	14 (13–15)	90 (82–98)

*Values in L $mmol^{-1}$ s^{-1}.

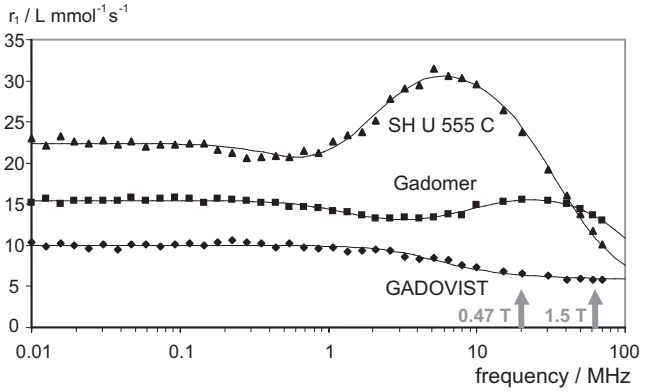

FIGURE 3. NMRD profiles for 3 selected MRI-CM (Gadomer, GADOVIST, SH U 555 C) in aqueous solution, normalized to 1 mmol/L at 30°C. On the logarithmic RF-frequency axis, the values corresponding to the field strengths of 0.47 T and 1.5 T, are indicated.

it can easily be seen from the NMRD profiles that relaxivity differences, as observed at 0.47 T, decrease with increasing field strengths. For all low molecular-mass Gd chelates with negligible protein binding, (eg, GADOVIST), the highest relaxivity was always found at lower field strengths. For this class of MRI-CM, continuously decreasing relaxivities were observed with increasing field strength. However, the NMRD profiles illustrate local maxima at medium field strength for the relaxivities of a macromolecular MRI-CM and a SPIO, as shown for Gadomer and SH U 555 C, chosen as examples in Figure 3. To appreciate the different conditions regarding sample temperature and magnetic field range compared with the other measurements, NMRD data were only considered as additional consistency check and for better qualitative visualization of local field-/frequency dependencies, within the given ranges.

Relaxivity values r_1 and r_2 as determined in water at magnetic field strengths of 0.47 T, 1.5 T, 3 T, and 4.7 T are summarized in Table 3, together with their individual error ranges. To visualize the relatively weak field strength dependence of relaxivities in water, the values obtained for the low molecular-mass Gd chelates are shown graphically in Figure 4.

Relaxivities in Plasma

Relaxivity values r_1 and r_2 as determined in plasma at magnetic field strengths of 0.47 T, 1.5 T, 3 T, and 4.7 T are summarized in Table 4, together with their individual error ranges. As opposed to the data measured in water, the field strength dependence of the values obtained in plasma for low molecular-mass Gd chelates was found to be more pronounced and is shown in Figure 5. Furthermore, it is clearly seen in Figure 5 that the differences of relaxivities between the MRI-CM in plasma decrease at higher magnetic field strengths. As illustrated previously (Fig. 4), this is not the case for the values measured in water.

Relaxivities in Blood

Measurements of relaxivities also were performed in whole blood at 1.5 T, which was done to investigate the comparability of the results within the framework of the experimental approach presented in this study. The results are shown in Table 5, together with their individual error ranges.

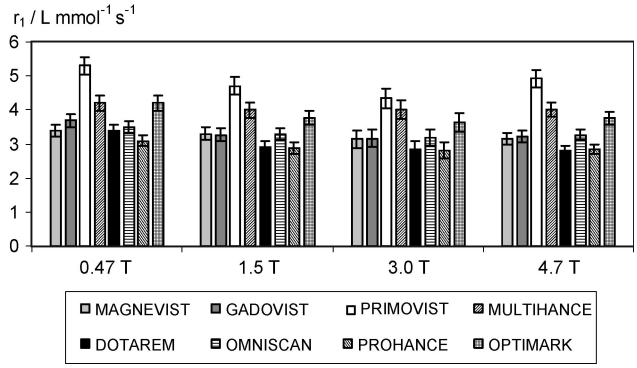

FIGURE 4. Relaxivities r_1 of low molecular-mass Gd chelates measured in water at 37°C at the field strengths of 0.47 T, 1.5 T, 3 T and 4.7 T.

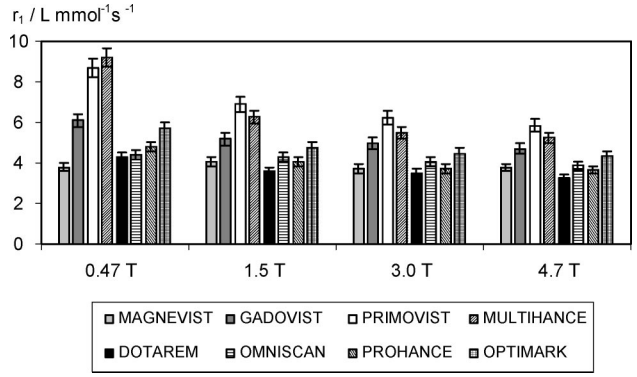

FIGURE 5. Relaxivities r_1 of low molecular-mass Gd chelates measured in bovine plasma at 37°C at the field strengths of 0.47 T, 1.5 T, 3 T and 4.7 T.

Comparison of the Results Obtained in Water, Plasma, and Whole Blood

Comparison of the data measured in plasma and in whole blood shows good agreement in r_1 for the Gd chelates within the given accuracy ranges. The transverse relaxivities (r_2), on the other hand, display moderate to considerable differences, in particular those of the SPIOs and the Mn chelate. For the SPIOs, this can be rationalized by the susceptibility effects on which the shortening of the relaxation times are based upon. The relaxivity differences found between bovine plasma and canine blood are small and we assume similar relaxivities in human blood, within the given error ranges.

A detailed analysis of the concentration dependence of the relaxivities, in particular for MRI-CM with considerable protein binding, was not within the scope of this experimental study. However, this issue has been addressed in the literature, for example, for MS-325 and for MULTIHANCE.[22,26–28,53] Limiting the CM concentration to a range between 0.25 mmol/L and 0.5 mmol/L and maintaining the serum albumin concentration in the physiological range of 3.5 g/dL to 5 g/dL, the variations of the measured relaxivity values do not exceed the accuracy ranges given in Tables 4 and 5. The situation may change, when protein-binding MRI-CM are present at very high concentrations, as occasionally obtained in vivo during the first pass after an i.v. bolus injection. Considering the protein bound state of such MRI-CM to exhibit a higher relaxivity than the unbound state, a higher concentration will lead to a decreased apparent relaxivity. However, to further elucidate the concentration dependence of the relaxivity of protein-binding MRI-CM, including concentrations in the high mM range, additional experimental investigations beyond the scope of this work would be required.

Field Strength Dependencies of r_1/r_2-Ratio

Apart from the absolute relaxivity values, various other parameters determine the signal intensity in CE-MRI. Some of these parameters are the intrinsic relaxation times of the tissue, the concentration of the contrast medium and a series of technical parameters that influence the signal intensity and hence the signal-to-noise (SNR) as well as the contrast-to-noise (CNR) ratios.

The basic equations describing the signal intensity for Spin-Echo and gradient-recalled-echo (GRE) sequences, include the respective dependencies on the T_1 and T_2 relaxation times:

$$SI_{SE} \propto (1 - e^{-TR/T_1})e^{-TE/T_2} \quad (5a)$$

$$SI_{GRE} \propto \sin\alpha \frac{(1 - e^{-TR/T_1})}{(1 - \cos\alpha\, e^{-TR/T_1})} e^{-TE/T_2^*} \quad (5b)$$

where the choice of the basic sequence parameters (TR, TE, flip angle α) determines the respective image weighting. Within the given context of basic considerations related to CE-MRI, other contrast weighting such as proton density and technically specific parameters are left aside.

Obviously, for T_1-weigthed MRI, signal-enhancement by CM is generally observed as long as the T_1-shortening (caused by r_1) is the dominant effect of the MRI-CM. However, the SI dependence on $TE/T_2^{(*)}$ expressed by Eq. (5) counteracts the signal increase in T_1-weighted CE-MRI at higher CM concentrations, where the condition $T_2^{(*)} \gg TE$ is no longer fulfilled. Hence, the achievable signal enhancement is under these conditions not only determined by the relaxivity r_1, but—via $T_2^{(*)}$—also by r_2. Therefore, in the limiting case of high CM concentrations (eg, in first pass CE-MRA), larger r_1/r_2 ratios can be favorable for T_1-weighted CE-MRI.[54]

Similar considerations apply for $T_2^{(*)}$-weighted MRI, where lower r_1/r_2 ratios can be advantageous in addition to high r_2 relaxivities.[55]

According to the different field strength dependencies of r_1 and r_2, respectively, the r_1/r_2 ratios decrease with increasing field strength. These alterations of r_1/r_2 ratios are more pronounced for SPIOs and protein-binding MRI-CM, than for Gd chelates without protein binding.

CONCLUSION

Comprehensive results of experimentally determined relaxivity values, measured at several magnetic field strengths and in different media, have been reported. All currently marketed MRI-CM in addition to 4 MRI-CM currently (ie, at the time of article submission) in clinical development have been included. Taking into account the problematic interlaboratory reproducibility and consistency of relaxivity measurements, this paper describes the relaxivity values for MRI contrast media, in a comparative study for the first time to such an extend. Error estimates were done based on individual standard errors of the T_1 and T_2 relaxation times. For Gd-based MRI-CM, satisfactory accuracy ranges of the calculated relaxivities were obtained, typically lying well within $\pm 6\%$ for r_1 and $\pm 15\%$ for r_2, respectively. Under the chosen experimental conditions, relaxivity data determined in plasma do not differ significantly from those obtained in whole blood within the same given accuracy ranges.

In conclusion, the individual dependencies of the relaxivities on the field strength for the 7 commercially available Gd-based MRI-CM (at the time of article submission) was found to be significantly different. Reflecting their different mode of action, relaxivity alterations were larger for those compounds exhibiting protein binding. The most pronounced decrease of r_1 relaxivity in plasma, as observed for one MRI-CM between 0.47 T and 3 T, was 40%, whereas the smallest observed change in r_1 was lying merely within the error range of $\pm 6\%$.

Considering the same group of Gd-based MRI-CM, their relaxivity differences at 0.47 T of up to 142%, decrease to 75% at 1.5 T and further to 57% at 3 T. As a consequence of the pronounced relaxivity deviations found between aqueous solutions and plasma and furthermore due to their significant field strength dependence, we strongly suggest to use values obtained in plasma at the field strengths of interest (currently, mainly 1.5 T and 3 T). According to the measurements and results from this study, it is recommended that relaxivity values determined in water and/or at 20 MHz (0.47 T) be avoided, if not required for specific investigations.

ACKNOWLEDGMENTS

The authors like to thank Mr. R. Gottberg (Schering AG, Berlin) for the NMRD measurements and Mrs. M. Narazaki (Nihon Schering) for relaxation time measurements at 4.7 T.

REFERENCES

1. Weinmann H-J, Brasch RC, Press WR, et al. Characteristics of gadolinium-DTPA complex: a potential NMR contrast agent. *Am J Roentgenol*. 1984;142:619–624.
2. Claussen C, Laniado M, Schorner W, et al. Gadolinium-DTPA in MR imaging of glioblastomas and intracranial metastases. *AJNR Am J Neuroradiol*. 1985;6:669–674.
3. Carr DH, Brown J, Bydder GM, et al. Intravenous chelated gadolinium as a contrast agent in NMR imaging of cerebral tumours. *Lancet*. 1984;1:484–486.
4. Runge VM, Carollo BR, Wolf CR, et al. Gd DTPA: a review of clinical indications in central nervous system magnetic resonance imaging. *Radiographics*. 1989;9:929–958.
5. Runge VM, Wells JW. Update: safety, new applications, new MR agents. *Top Magn Reson Imaging*. 1995;7:181–195.
6. Magerstadt M, Gansow OA, Brechbiel MW, et al. Gd(DOTA): an alternative to Gd(DTPA) as a T1, 2 relaxation agent for NMR imaging or spectroscopy. *Magn Reson Med*. 1986;3:808–812.
7. Van Wagoner M, O'Toole M, Quay SC. Nonionic magnetic resonance imaging contrast agents. Clinical trial experience of safety, tolerance, and efficacy of gadodiamide injection. *Invest Radiol*. 1990;25(Suppl 1):S39–41.
8. Runge VM, Armstrong MR, Barr RG, et al. A clinical comparison of the safety and efficacy of MultiHance (gadobenate dimeglumine) and Omniscan (gadodiamide) in magnetic resonance imaging in patients with central nervous system pathology. *Invest Radiol*. 2001;36:65–71.
9. Runge VM, Dean B, Lee C, et al. Phase III clinical evaluation of Gd-HP-DO3A in head and spine disease. *J Magn Reson Imaging*. 1991;1:47–56.
10. Adzamli K, Periasamy MP, Spiller M, et al. NMRD assessment of Gd-DTPA-bis(methoxyethylamide), (Gd-DTPA-BMEA), a nonionic MRI agent. *Invest Radiol*. 1999;34:410–414.
11. Grossman R, Kuhn MJ, Maravilla K, et al. Multicenter evaluation of the safety, tolerance, and efficacy of OptiMARK in magnetic resonance imaging of the brain and spine. *Acad Radiol*. 1998;5(Suppl 1):S154–155; discussion S156.
12. Vogler H, Platzek J, Schuhmann-Giampieri G, et al. Pre-clinical evaluation of gadobutrol: a new, neutral, extracellular contrast agent for magnetic resonance imaging. *Eur J Radiol*. 1995;21:1–10.
13. Tombach B, Heindel W. Value of 1.0-M gadolinium chelates: review of preclinical and clinical data on gadobutrol. *Eur Radiol*. 2002;12:1550–1556.
14. Earls JP, Bluemke DA. New MR imaging contrast agents. *Magn Reson Imaging Clin N Am*. 1999;7:255–273.
15. Weinmann HJ, Ebert W, Misselwitz B, et al. Tissue-specific MR contrast agents. *Eur J Radiol*. 2003;46:33–44.
16. Taupitz M, Wagner S, Schnorr J, et al. Phase I clinical evaluation of citrate-coated monocrystalline very small superparamagnetic iron oxide particles as a new contrast medium for magnetic resonance imaging. *Invest Radiol*. 2004;39:394–405.
17. Kellar KE, Fujii DK, Gunther WH, et al. NC100150 Injection, a preparation of optimized iron oxide nanoparticles for positive-contrast MR angiography. *J Magn Reson Imaging*. 2000;11:488–494.
18. Elizondo G, Fretz CJ, Stark DD, et al. Preclinical evaluation of MnDPDP: new paramagnetic hepatobiliary contrast agent for MR imaging. *Radiology*. 1991;178:73–78.
19. Hamm B, Vogl TJ, Branding G, et al. Focal liver lesions: MR imaging with Mn-DPDP—initial clinical results in 40 patients. *Radiology*. 1992; 182:167–174.
20. Bloembergen N, Morgan LO. Proton relaxation times in paramagnetic solutions. Effects of electron spin relaxation. *J Chem Phys*. 1961;34: 843–850.
21. Lauffer RB. Metal complexes as water proton relaxation agents for NMR imaging: theory and design. *Chem Rev*. 1987;87:901–927.
22. Caravan P, Ellison JJ, McMurry TJ, et al. Gadolinium(III) Chelates as MRI contrast agents: structure, dynamics, and applications. *Chem Rev*. 1999;99:2293–2352.
23. Banci L, Bertini I, Luchinat C. *Nuclear and Electron Relaxation: The Magnetic Nucleus-Unpaired Electron Coupling in Solution*. Weinheim: VCH; 1991.
24. Bertini I, Luchinat C. NMR of Paramagnetic Substances. *Coord Chem Rev*. 1996;150:1–292.
25. Schuhmann-Giampieri G, Schmitt-Willich H, Press WR, et al. Preclinical evaluation of Gd-EOB-DTPA as a contrast agent in MR imaging of the hepatobiliary system. *Radiology*. 1992;183:59–64.
26. Kirchin MA, Pirovano GP, Spinazzi A. Gadobenate dimeglumine (Gd-BOPTA). An overview. *Invest Radiol*. 1998;33:798–809.
27. Caravan P, Cloutier NJ, Greenfield MT, et al. The interaction of MS-325 with human serum albumin and its effect on proton relaxation rates. *J Am Chem Soc*. 2002;124:3152–3162.
28. Cavagna FM, Maggioni F, Castelli PM, et al. Gadolinium chelates with weak binding to serum proteins. A new class of high-efficiency, general purpose contrast agents for magnetic resonance imaging. *Invest Radiol*. 1997;32:780–796.
29. EMRF (European Magnetic Resonance Forum Foundation) Recommendations for the nomenclature of MR imaging contrast agent terms. *Acta Radiol.* 1997;38:5.
30. Niendorf HP, Laniado M, Semmler W, et al. Dose administration of gadolinium-DTPA in MR imaging of intracranial tumors. *AJNR Am J Neuroradiol*. 1987;8:803–815.
31. Rinck PA, Muller RN. Field strength and dose dependence of contrast enhancement by gadolinium-based MR contrast agents. *Eur Radiol*. 1999;9:998–1004.
32. Haustein J, Laniado M, Niendorf HP, et al. Administration of gadopentetate dimeglumine in MR imaging of intracranial tumors: dosage and field strength. *AJNR Am J Neuroradiol*. 1992;13:1199–1206.
33. Elster AD. How much contrast is enough? Dependence of enhancement on field strength and MR pulse sequence. *Eur Radiol*. 1997;7(Suppl 5): 276–280.
34. Reimer P, Muller M, Marx C, et al. T1 effects of a bolus-injectable superparamagnetic iron oxide, SH U 555 A: dependence on field strength and plasma concentration–preliminary clinical experience with dynamic T1-weighted MR imaging. *Radiology*. 1998;209:831–836.
35. Bjerner T, Johansson L, Wikstrom G, et al. In and ex vivo MR evaluation of acute myocardial ischemia in pigs by determining R1 in steady state after the administration of the intravascular contrast agent NC100150 injection. *Invest Radiol.* 2004;39:479–486.
36. Donahue KM, Burstein D, Manning WJ, et al. Studies of Gd-DTPA relaxivity and proton exchange rates in tissue. *Magn Reson Med*. 1994;32:66–76.
37. Judd RM, Reeder SB, May-Newman K. Effects of water exchange on the measurement of myocardial perfusion using paramagnetic contrast agents. *Magn Reson Med*. 1999;41:334–342.
38. Goyen M, Herborn CU, Vogt FM, et al. Using a 1 M Gd-chelate (gadobutrol) for total-body three-dimensional MR angiography: preliminary experience. *J Magn Reson Imaging*. 2003;17:565–571.
39. Huppertz A, Rohrer M. Gadobutrol, a highly concentrated MR-imaging contrast agent: its physicochemical characteristics and the basis for its use in contrast-enhanced MR angiography and perfusion imaging. *Eur Radiol*. 2004;14(Suppl 5):M12–M18.
40. Herborn CU, Lauenstein TC, Ruehm SG, et al. Intraindividual comparison of gadopentetate dimeglumine, gadobenate dimeglumine, and gadobutrol for pelvic 3D magnetic resonance angiography. *Invest Radiol*. 2003;38:27–33.
41. Fink C, Puderbach M, Ley S, et al. Contrast-enhanced three-dimensional pulmonary perfusion magnetic resonance imaging: intraindividual comparison of 1.0 M gadobutrol and 0.5 M Gd-DTPA at three dose levels. *Invest Radiol*. 2004;39:143–148.
42. Ibrahim MA, Emerson JF, Cotman CW. Magnetic resonance imaging relaxation times and gadolinium-DTPA relaxivity values in human cerebrospinal fluid. *Invest Radiol*. 1998;33:153–162.
43. Mandry D, Pedersen M, Odille F, et al. Renal functional contrast-enhanced magnetic resonance imaging: evaluation of a new rapid-clearance blood pool agent (p792) in Sprague–Dawley rats. *Invest Radiol*. 2005;40:295–305.

44. Murphy PS, Leach MO, Rowland IJ. The effects of paramagnetic contrast agents on metabolite protons in aqueous solution. *Phys Med Biol*. 2002;47:N53–N59.
45. Schnorr J, Wagner S, Abramjuk C, et al. Comparison of the iron oxide-based blood-pool contrast medium VSOP-C184 with gadopentetate dimeglumine for first-pass magnetic resonance angiography of the aorta and renal arteries in pigs. *Invest Radiol*. 2004;39:546–553.
46. Muller RN, Gillis P, Moiny F, et al. Transverse relaxivity of particulate MRI contrast media: from theories to experiments. *Magn Reson Med*. 1991;22:178–182; discussion 195–196.
47. Knopp MV, von Tengg-Kobligk H, Floemer F, et al. Contrast agents for MRA: future directions. *J Magn Reson Imaging.* 1999;10:314–316.
48. Vander Elst L, Laurent S, Muller RN. Multinuclear magnetic resonance characterization of paramagnetic contrast agents. The manifold effects of concentration and counterions. *Invest Radiol*. 1998;33:828–834.
49. Craik DJ, Levy GC. Factors affecting Accuracy in 13C Spin-Lattice Relaxation Measurements. In: Levy GC, ed. *Topics in Carbon-13 NMR Spectroscopy*. New York: Wiley; 1984;239–274.
50. Carrington A, McLachlan AD. *Introduction to Magnetic Resonance with Applications to Chemistry and Chemical Physics*. New York: Harper & Row; 1979.
51. Farrar TC, Becker ED. *Pulse and Fourier Transform NMR*. New York: Academic Press; 1971.
52. Fullerton GD, Potter JL, Dornbluth NC. NMR relaxation of protons in tissues and other macromolecular water solutions. *Magn Reson Imaging*. 1982;1:209–226.
53. de Haen C, Calabi L, La Ferla R. The problematic determination of proton magnetic relaxation rates of protein-containing solutions. *Acad Radiol.* 2002;9(Suppl 1):S2–S4.
54. Weinmann HJ, Bauer H, Ebert W, et al. Comparative studies on the efficacy of MRI contrast agents in MRA. *Acad Radiol.* 2002;9(Suppl 1): S135–136.
55. Bjornerud A, Johansson LO, Ahlstrom HK. Renal $T_2^{(*)}$ perfusion using an iron oxide nanoparticle contrast agent–influence of T_1 relaxation on the first-pass response. *Magn Reson Med*. 2002;47:298–304.